EurJIC
European Journal of Inorganic Chemistry

Minireview
doi.org/10.1002/ejic.202000629

Nanoparticle-Based Electronics

Integration of Individual Functionalized Gold Nanoparticles into Nanoelectrode Configurations: Recent Advances

Silvia Karthäuser,[a] Sophia Peter,[b] and Ulrich Simon*[b]

Abstract: Chemically synthesized gold nanoparticles (AuNPs) have attracted much interest for application in various technologically relevant fields including nanoelectronics. In this particular research area, the most promising approach to take full advantage of the tunability in size, shape, and ligand composition of nanoparticles is the integration of a well-defined number of AuNPs into a nanoscale device. This short review highlights recent progress in the introduction of AuNP into nanoelectronic circuitry by means of selected examples, that demonstrate a "proof-of-concept". Synthetic concepts to obtain isotropic and Janus-like particles as well as lithographic techniques that allow for the fabrication of nanoelectrode structures, which enable the electrical addressing of individual nanoparticles, are presented. A particular focus of this work is the question of how distinct molecular properties can be addressed in a technologically applicable device geometry by controlling the molecular functionalities in the proximity of semiconductor technology.

1. Introduction

Today, chemically synthesized metallic nanoparticles (NPs) are well-established in various fields of research, ranging from catalysis via optoelectronics to medicine.[1] Their synthesis is in many cases straightforward and a plethora of protocols have been developed for tuning their shape and size up to the level of atomic precision. Among such inorganic NPs, gold nanoparticles (AuNPs) play a particularly dominant role, propelled by their high chemical stability, their versatile surface chemistry and their fascinating optical properties. The latter is most impressively noticeable by means of the surface plasmon resonance, which e.g. is responsible for the typical red color of AuNPs in colloidal dispersion.

AuNPs can be synthesized in aqueous solution as well as in organic solvents and can be functionalized with various organic molecules, often described as ligands. Such ligands can form bonds coordinatively as electron donors (Lewis bases), or via van der Waals forces to surface atoms of the NPs (Lewis acid).[2] The ligand-to-metal binding strength depends on the number of anchoring groups per ligand[3] and the nature of the respective electron donor groups. The latter can, for example, be carboxylic acids, amines, phosphines or thiols, whereas the binding strength follows the order O < N < P < S, according to Pearsons Hard and Soft Acids and Bases (HSAB) concept. The ligands, in first approximation, coat the particles isotropically and their function is twofold: First, they prevent particle aggregation in solution via electrostatic and/or steric stabilization depending on their solubility limit and extrinsic factors, such as ionic strength or temperature of the solvent. Second, they bring another chemical and/or physical functionality that is intrinsic to the ligand to the surface of the particles, e.g. charge, polarity, or an additional optical addressability. Recent advances in AuNP chemistry can break symmetry of isotropic functionalization so that "patchy" or "Janus-like" particles are now accessible, providing directionality in function and binding.[4]

When AuNPs are assembled to one-, two- or three-dimensional superstructures or when simply transferred to the dried state by solvent evaporation, these ligands serve not only as "spacers", but can even dictate the integral physical properties of the overall AuNP-ligand system. Thus, they play a fundamental role in the structure formation and the electron transport properties.

The application potential for AuNPs in nanoelectronics was already noticed in the early 1990s.[5] However, at this time the focus was on single electron charging effects utilizing the size dependence of the Coulomb charging energy to eventually rise the operation temperature of single electron devices up to the level of room temperature. In most cases, the stabilizing ligands were mainly considered as dielectric spacers surrounding the metal cores, mostly irrespective of their chemical nature and of the possibility to exploit their intrinsic functionality in devices.

In the following, we will provide a few of the manifold examples for charge transport properties of ensembles as well as of

[a] Dr. S. Karthäuser
Peter Grünberg Institut (PGI-7) and JARA-FIT, Forschungszentrum Jülich GmbH,
Jülich 52425, Germany
[b] S. Peter, Prof. Dr. U. Simon
Institute of Inorganic Chemistry and JARA-FIT, RWTH Aachen University, Aachen 52074, Germany
E-mail: ulrich.simon@ac.rwth-aachen.de
ORCID(s) from the author(s) for this article is/are available on the WWW under https://doi.org/10.1002/ejic.202000629.

Part of the German Chemical Society ADUC Prizewinner Collection

individual AuNPs dominated by Coulomb charging energy. For instance, Pileni et al. discussed signatures of single particle properties and three dimensional charge transport in tunneling spectroscopy measurements on micellar-stabilized 4.3 nm silver nanoparticles.[5d,6] While single particles revealed a Coulomb blocking state expressed by a threshold voltage in current-voltage (*I*/*U*) characteristics, the Coulomb gap almost vanishes in the three-dimensionally packed particles due to the coupling of the electron states in the close-packed system.

Furthermore, temperature and field dependent DC and AC electrical transport measurements of densely packed, ligand-stabilized 1.4 nm AuNPs showed that a thermally activated, stochastic, multiple site hopping process dominates over a wide temperature range. Here, the AuNPs serve as localization sites for individual electrons, which are "embedded" in a dielectric matrix, i.e. the ligand shell.[7]

For arrays of 1.6 nm AuNP, electrical transport properties resembled that of a weakly coupled molecular solid which is comprised of discrete, nanoscaled metallic islands separated by insulating ligand barriers.[8] The integral properties are thus mainly determined by the single electron charging energy of the individual AuNPs, which in turn is governed by the particle diameter, the dielectric properties of the passivating ligands, the classical electrostatic coupling between neighboring cores, and the interparticle resistance, arising from the insulating nature of the stabilizing ligands that separate the metal cores.

Alivisatos et al. managed to electrically address individual immobilized 5.8 nm Au nanoparticle from solution inside a nanoelectrode gap.[9] By measuring the *I*/*U* characteristic at 77 K, classical Coulomb blockade effects could be observed. Sato et al. conducted first experimental attempts in order to build up a single electron transistor formed by ca. 15 nm AuNPs trapped in a 30 nm electrode gap. At 4.2 K, the device showed clear Coulomb staircases and periodic conductance oscillations in dependence of the gate voltage. Again, the organic molecules (1,6-hexanedithiol) acted as spacers between the particles and the particle electrode interface, providing tunnel barriers for the voltage driven electron transport.[10] Furthermore, Majima et al. very recently introduced a passivated, chemically assembled single-electron transistor (SET) based on decanethiol-stabilized 6.2 nm AuNPs, serving as Coulomb islands. They were able to demonstrate three-input gate logic operations by using a device with multiple gates separated by organic or organic/inorganic hybrid passivation layers from the Coulomb island.[11]

However, new functionalities may arise if organic molecules are applied as stabilizing ligands, which already have proven rectifying or switching behavior in highly sophisticated devices in vacuo or at cryogenic temperatures at the single molecule level, in molecular monolayers or large scale thin film devices.[12] For example, if switchable organic molecules interlinking two-dimensional close-packed arrays of metallic nanoparticles can change their conformation, charge state, or properties like the conductivity upon external stimuli, the macroscopic properties of such arrays will become tunable. Such assemblies can be rather flexible platforms to study the electronic and plasmonic coupling, which is of fundamental interest in chemistry and physics.[13] Furthermore, the formation of such superstructures has opened an avenue into various applications that include biological and chemical sensors, pressure sensors, catalytic coatings, or nanoelectronic devices down to the level of single electron transistors.[14]

Hence, in order to take full advantage of the tunability in size, shape, and ligand composition of NPs in such applications and explore their potential for further developments, integra-

Ulrich Simon currently holds a Full Professorship and Chair at the Institute of Inorganic Chemistry at RWTH Aachen University in Germany. He was born and raised in Essen, Germany. He studied Chemistry at the University of Essen, where he also undertook his doctoral research in solid state chemistry. Since 2000 he has been Professor at the RWTH Aachen University. His research program is focused on the electron-functional and biofunctional properties of chemically designed nanostructures.

Silva Karthäuser is leader of the molecular electronics group in the institute of Professor Waser at the Peter Grünberg Institute (PGI-7, Electronic Materials), Forschungszentrum Jülich in Germany. She received her Ph.D. in physical chemistry from the Technical University Darmstadt, Germany. In 1987 she joined the AGFA-Gevaert GmbH in Leverkusen, where she developed sub-micrometer particles for color negative materials. In 2002 she moved to the FZJ. Her current research includes nanoelectronic test devices, charge transport through hybrid structures and addressing molecules by external triggers.

Sophia Peter was born and raised in Düsseldorf. She received her Master degree at the RWTH Aachen University and is currently working on her Ph.D. in the research group of Professor Ulrich Simon. Her research interest includes synthesis and characterization of ruthenium terpyridine gold nanoparticle hybrids.

Minireview
doi.org/10.1002/ejic.202000629

tion of a controlled number of well-defined AuNPs into a nanoscale device concept is vital. This particularly holds true for nanoelectronic applications, which require:
(i) a fabrication technique to produce nanoelectrode structures with electrode gaps complementary to the NP size
(ii) functionalization of NPs with molecules bearing tailored electronic properties and allowing a high degree of control over contact formation with the solid-state electrodes, and
(iii) integrating NP-ligand systems in such nanoelectrode configurations in a reproducible and reliable manner.

Only the combination of these crucial steps will enable control over the charge transfer through the formed nanoscale molecule-NP device and will allow the selective addressing of intrinsic molecular functionalities.

As soon as these goals are met, molecular electronics is expected to have major impact on prospective nanoelectronic applications, as molecularly-defined device functionalities, such as molecular rectifiers[15] or nanoparticulate memristors[16] that go beyond the properties of single electron transistors, would come into reach.[17] Moreover, in our envisioned approach multiple electronic functionalities are integrated in one single AuNP device and thus, unique miniaturization possibilities become available. This could be achieved by combining sophisticated integration technology with the intrinsic functionality of single molecules. Therefore, our device concept is based on Janus-type metal nanoparticles immobilized between heterometallic nanoelectrodes in a directed way and thus, forming a rectifier. Furthermore, one half-shell of the Janus-like AuNPs will be formed, for example, by optically and/or electronically addressable molecules in the order to establish a switching unit. The second half-shell can be used to adjust the device conductance or to introduce another functionality. Thus, a robust prototypical device will be created in the proximity to semiconductor technology. At the same time these single Janus nanoparticle devices will be suitable as interface to a chemical or biological environment and have the potential to sense external perturbations like pH values, different gas environments, and electric, electromagnetic or magnetic fields. Although it is not likely that molecular electronics will replace present-day silicon-based technology in the foreseeable future, it will enable to add a plethora of additional functionalities to it.

With this short review, we illustrate recent progress in the design, the synthesis and the functional properties of AuNPs and in their integration into nanoelectronic circuitry. After a short tutorial-style discussion of the synthetic concepts to couple molecular ligands to AuNPs in order to form isotropic and

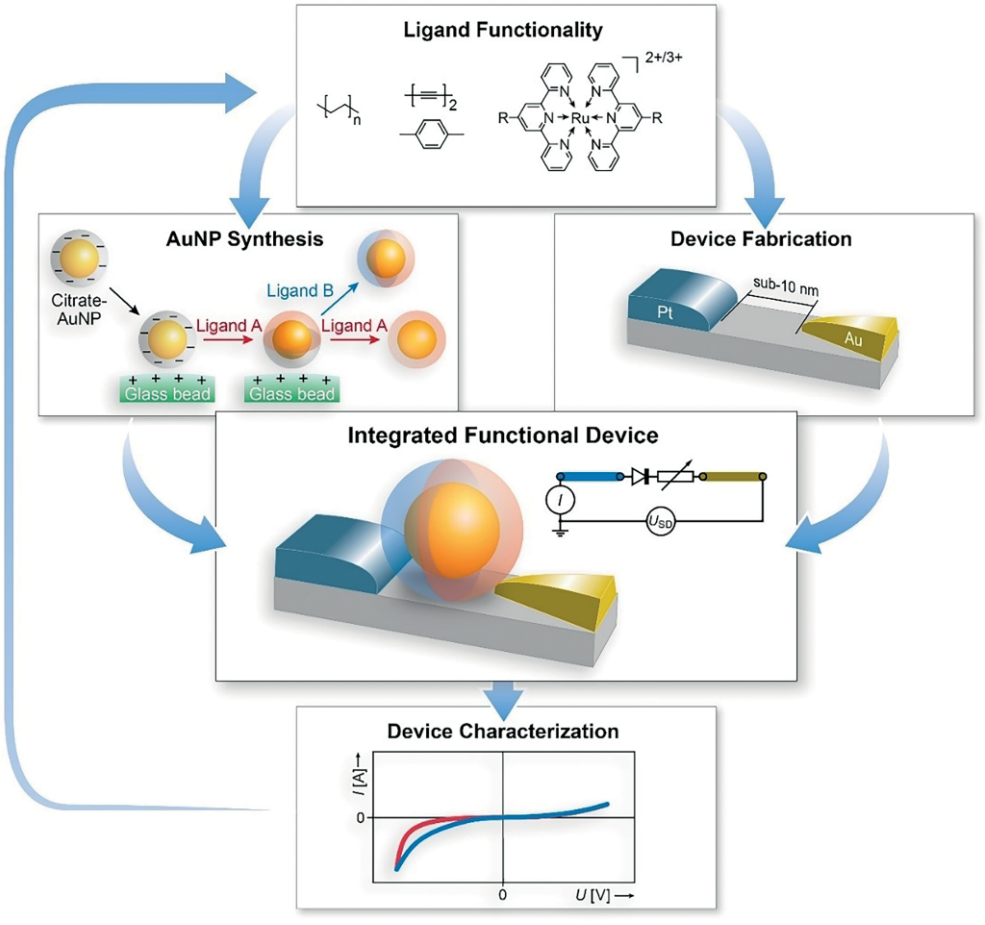

Figure 1. Schematic illustration of the concept of integrating individual AuNPs with tailored functionalization into nanoelectrode configurations, comprising the ligand design, the synthesis of functionalized AuNPs, the fabrication of nanoelectrode devices, and the electrical characterization of the device with integrated AuNP by recording the current *I* as a function of the applied source-drain voltage *U*.

Janus-like particles, we will introduce the lithographic techniques that allow for fabrication of nanoelectrode structures, which enable the electrical addressing of individual nanoparticles. We will acquaint the reader with the principles of functionalization by means of selected literature examples mainly taken from our recent work of the last decade. These include molecules serving as molecular wires or switches, directed immobilization in order to introduce asymmetry into the device, and specifically double-barrier tunnel junctions which have a tremendous impact on the charge transport behavior. Thereby, we pay special attention to how distinct molecular properties can be addressed in a technologically applicable device geometry by controlling the molecular functionalities in the proximity of semiconductor technology. We will discuss the individual prerequisites particle-wise and device-wise to achieve this goal and we illustrate the sub-ordinate targets that need to be met toward the integration with the following scheme (Figure 1).

Finally, based on these "proof-of-concept" studies, we will give a tentative evaluation of which opportunities may arise, which challenges and limitations are foreseeable, and which future directions may be envisaged for the further development of the field of nanoelectronics.

2. Synthesis of Isotropically and Anisotropically Functionalized Gold Nanoparticles

2.1. Synthesis of Gold Nanoparticles

A monodisperse size distribution of AuNPs is essential for their implementation in nanoelectronic devices. While numerous reviews and articles deal with the synthesis, characterization and properties of AuNPs in all sizes and morphologies,[1b,1d,18] this minireview focuses on the functionalization of spherical, monodisperse AuNPs in a size range of 10 to 15 nm. Citrate-stabilized AuNPs of defined sizes can be reproducibly synthesized applying the Turkevich method.[19] The synthesis is based on the reduction of $HAuCl_4$ by citrate in aqueous media. Citrate functions as the reducing agent and as stabilizing but weakly binding ligand, which can readily be exchanged by various types of stronger ligands i.e. thiols, phosphines, amines.[1b,18a]

2.2. Isotropic and Anisotropic Functionalization

The controlled functionalization of citrate stabilized AuNP can be achieved through different approaches. However, prior to synthesis an elaborate selection of the respective ligands has to be made with respect to their envisaged function.

As already mentioned, the ligands surrounding the AuNP hold two functions: the stabilization of the AuNP and the addition of functionality. The stabilization of AuNP can be carried out according to two basic concepts – steric or electrostatic stabilization.[20] Steric stabilization is based on a lower entropy and the rise of the osmotic pressure between sterically demanding ligands i.e. polymers or long-chain alkyls. Electrostatic stabilization can be achieved by a charged ligand shell, such as amine or carboxylate ligands that offer electrostatic stabilization when being protonated or deprotonated, respectively. This provides an elegant method to control the degree of stabilization by the pH of the solvent. Amines result in a positive surface charge in acidic media, while carboxylates result in a negative surface charge in basic media.[21] The charged ligand shells surrounding the AuNP are compensated by counterions in the solution, thus forming an electric double layer comprising a compact and a diffuse region. The thickness of the diffuse part of the electric double layer is determined by the concentration of ions in the solution. A thicker diffuse region results if the ion concentration is low.

With a rising size of NP the aggregation barrier of the AuNP rises, while the rise in ion concentration lowers the barrier for aggregation.[20] This effect is also dependent on the nature of the respective ions. Hofmeister ranked anions and cations according to their participation behavior. Those ions were named according to their ability to structure water, meaning ions strongly binding water were called kosmotopic, while ions weakly binding water were called chaotopic.[22] These factors will influence the binding to the electrode structures since kosmotopic ions as counterions will probably integrate water molecules into the ligand shell.

In the past molecules containing carboxylic acids or amines as terminating groups have been used as capping agents that allow biological and medical applications.[21e,23] In addition, properties like the pH-dependent protonation/deprotonation enable specific binding properties of these anchoring groups to charged electrode surfaces.[4b,21a–21c,24] Therefore, ligands like 1,8-mercaptooctanoic acid (MOA), 1,8-aminooctanethiol (AOT) and 1-mercapto-11-undecyl tetra-(ethylene glycol) (MUTEG) are interesting candidates for functionalization experiments. For the synthesis of isotropic AuNPs with these ligands, citrate is exchanged by an excess of MOA or MUTEG as a straightforward approach (Figure 2, bottom).[21e,24b,25] The excess of the ligand and the exchanged citrate is removed afterwards by centrifugation. The synthesis of AOT-functionalized AuNPs can be reached through a solid phase supported synthesis reported by Nath et al.[24b,26] pH-dependent UV/Vis measurements proved that MOA-AuNP are stable in alkaline buffer solutions, while the AOT are stable in acidic buffer solutions. This can be explained by the deprotonation and protonation of carboxylic acids and amines in the respective buffer solutions, enabling in both cases an electrostatic stabilization of the functionalized AuNPs. The corresponding surface charge of MOA-AuNPs under those conditions is negative, while it is positive for AOT-AuNPs.[24b]

Beside the binding properties, the conductivity of ligands is important for application in molecular electronics. Molecules based on aromatic backbones, like mercaptophenylamine (MPA), provide higher conductivity than alkane derivatives (AOT) while perpetuating the same pH-dependent properties. MPA-stabilized AuNPs have been synthesized and investigated as calorimetric sensors for explosives.[27] MPA-AuNPs can further be synthesized according to the synthesis of AOT-AuNPs (see Figure 2 for structure). The protonation of the ligand also leads to single AuNPs, as they are sufficiently shielded through electrostatic stabilization.[24a]

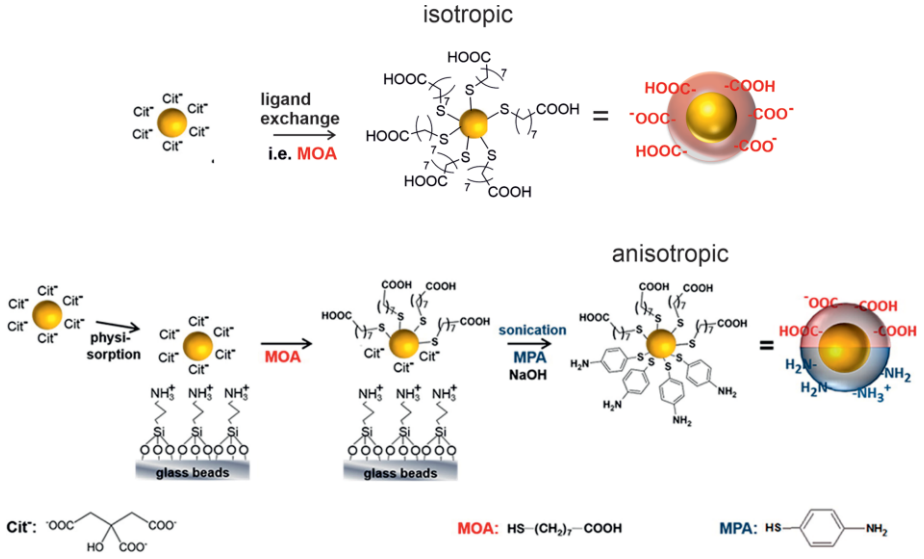

Figure 2. Functionalization by ligand exchange (isotropic, top). Preparation scheme of Janus-type AuNPs (anisotropic, bottom). AuNP capping layers: Cit^- (sodium citrate), MOA (red, 1,8-mercaptooctanoic acid), and MPA (blue, 4-mercaptophenylamine). Adapted with permission from ref.[24a] Copyright (2014) American Chemical Society.

Anisotropic Janus-type AuNPs are primarily studied in terms of their amphiphilic character as analogue to surfactant molecules,[28] or application in catalysis,[29] emulators[30] and self-assembly.[4a,28,31] Those amphiphilic AuNPs can be synthesized combining ligands that are dissolved in different immiscible media (organic vs. aqueous solutions) forming a phase boundary.[28,32] However, in order to synthesize Janus-type AuNPs with two kinds of hydrophilic ligands another approach has to be followed. In this case, it is necessary to shield one side of the particle while the ligands of the opposite side are exchanged with the desired ligand (Figure 2, top).[28] Janus-type AuNPs can be synthesized in a similar approach to Shumaker-Parry et al. and by the same preparation method as mentioned for the isotropic AOT-AuNPs by Nath et al.[26,33] However, instead of adding the same ligand, when the AuNPs are detached from the glass surface, another ligand can be introduced to synthesize Janus-like AuNPs (Figure 2, bottom). Janus-like AuNPs in aqueous solution functionalized with e.g. MPA and MOA are already stable at neutral pH and thus comprise the same pH-dependent properties of the respective MPA and MOA stabilized isotropic AuNPs. ζ-potential measurements in neutral conditions reveal a negative surface charge of –32.5 ± 8.7 mV.[24a] As the amine-metal binding energy is considerably different for specific metals, MPA or AOT ligands provide the possibility to direct the assembly of Janus-AuNPs between heterometallic nanoelectrodes.[4b,21b,24b,34]

Another kind of Janus-like AuNPs can be synthesized with a liquid-liquid approach adopted from Andala[32b] and Ciesa.[32a] For that 1-octanethiol (OT) and MOA ligands are added to a mixture of water and toluene with citrate-stabilized AuNPs. The AuNPs can align along the phase boundary and on the surface of the reaction tube made of polypropylene, thus enabling the exchange of ligands on both hemispheres selectively. Removing both solvents with excess ligands through rinsing with fresh solvent makes it possible to purify the AuNPs. Adding new solvent leads to an alignment at the phase boundary again, which offers the possibility to transfer the Janus-like AuNPs onto a substrate in a highly ordered manner.[4b]

While MOA, AOT and MPA ligands sufficiently stabilize AuNPs, certain ligands have the potential to add functionality to an envisaged AuNP-based nanodevice. To enhance charge transport properties of ligands, their backbone should be based on a delocalized electron system.[35] Another approach, to enhance the stability of the ligand shell surrounding AuNPs, was introduced by Kanaras et al. Here, diacetylene (DA) ligands were polymerized by UV irradiation.[36] The polymerization led to a network of conjugated double and triple bonds along the ligand shell and resulted in an extraordinary high stability of the AuNPs.

Chen et al. synthesized 5 nm Janus-type AuNPs with a suitable ligand (3,5-octadiyne-1-ol-8-thiol). However, this ligand cannot facilitate full polymerization of the shell.[37] In order to allow full polymerization, a DA ligand can be designed with a spacer length of five CH_2 units ensuring a full conjugation of the ligand shell, while obtaining a promising length for molecular electronics.[21d] Straightforward ligand exchange of citrate-stabilized AuNP with this ligand is possible in neutral pH conditions. Those AuNP exhibit an extraordinary high stability against ions, displacement reactions and temperature.[21d]

NPs functionalized with 2,2′:6′,2″-terpyridines (TP) have been discussed in detail by Winter et al.[38] The TP function has a strong binding affinity to transition and rare earth metal ions, which leads to an extensive interest in various scientific areas.[39] The employed AuNP – following Brust-like approaches or other small colloidal AuNP synthesis – show sizes between 1.6 and 5 nm.[39k,40] As a conductive and redox-active molecule that binds to AuNPs through a thiol group, 4′-(4-mercaptophenyl)-2,2′:6′,2″-terpyridine (MPTP) has a large potential for molecular electronics.[39i,40b,41] MPTP-AuNPs with a size of

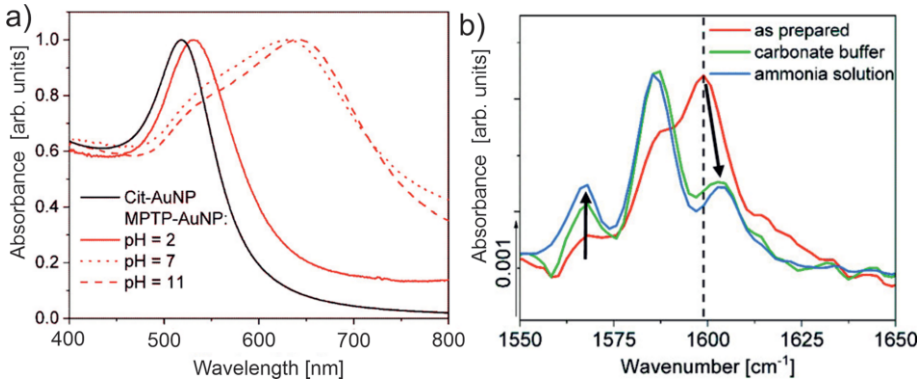

Figure 3. pH-dependent behavior: (a) UV/Vis of MPTP-AuNPs in solution, (b) IRRAS of MPTP-AuNP immobilized on a Au surface. Adapted with permission from ref.[24c] Copyright (2019) American Chemical Society.

Figure 4. Schematic illustration of the Ru(MPTP)(MPTP-SAc)-AuNP synthesis.[24d] Reprinted with permission from ref.[24d] Copyright (2020) American Chemical Society.

15 nm, which makes them suitable to be integrated into electron beam lithographically fabricated nanoelectrodes, can be obtained through ligand exchange in acidic conditions.[24c] The pH-dependent UV/Vis and IRRAS measurements reveal, that MPTP-AuNPs are primarily stable in acidic conditions and that their IR absorption is directly correlated to the protonation state (Figure 3).[24c] According to Nakamoto et al. the protonation of the MPTP causes a conformation change of the pyridine rings from *trans-trans* to *cis-cis* in the protonated state.[42] Furthermore, those MPTP-AuNPs hold the potential to build switchable complexes with ruthenium (Ru).[24b,24c,43] Recently, sub-5 nm RuTP-AuNPs were prepared that exhibit redox-switchable and photo-active properties with a high potential for various applications.[39k,40c,44] In a similar approach to Ito et al., 15 nm MPTP-AuNPs were heated together with an active Ru precursor in order to obtain Ru(MPTP)(MPTP-SAc)-AuNP (Figure 4).[24d]

The successful complexation can be shown by IR spectroscopy.[24d] An acetyl-protection (Ac) group for the second MPTP ligand enables the protection of the thiol group in order to avoid interlinking of AuNPs and to identify the successful complexation by IR spectroscopy. Just before binding to the electrodes the Ac group can be removed my ammonolysis.[45]

2.3. Directed and Selective Self-Assembly of Functionalized AuNP

Many approaches to assemble AuNPs in a directed or selective way have been followed in order to overcome scaling limitations of lithography techniques[46] and to study photo- or electrochemical, optical or structural properties.[47] Those approaches involve Langmuir–Blodgett techniques[48] and pH-dependent, chemically directed,[47a,33,47b,47c,49] DNA/biomolecule-templated, or polymer-mediated self-assembly methods.[50] All these methods have the directing properties of the ligands attached to the surface of AuNPs or substrates in common.

In order to assure binding of ligand molecules to the AuNP surface and electrodes, AuNP functionalized with self-assembled monolayers (SAM) and pH-sensitive molecules are promising candidates.[24b] Thiol ligands with terminating carboxylic acid or amine groups were an obvious choice as they i) ensure binding to the AuNP surface by S–Au bonding ii) have different affinity to charged surfaces[19d,21a,51] and iii) can be tuned by pH-adjustments.[21e,47a,52] For example, Janus-AuNP adsorb with the MOA or MPA hemisphere on positively or negatively charged self-assembled monolayers (SAMs) on Au, respectively (Figure 5). This principle can be adapted also to Janus-AuNPs with OT and MOA. They adsorb selectively on non-polar or polar SAMs (not shown). Directed immobilization is possible through hydrophilic/hydrophobic and electrostatic interaction. IRRAS measurements can specifically detect those ligands that are not shielded by the Au core and therefore prove the Janus character of the AuNPs.[4b]

Furthermore, directed self-assembly of AOT and MOA-AuNPs on AuPd and Pt surfaces can be shown by pH-dependent adsorption experiments. At a high ionic strength of HEPES buffer (0.02 M) the positively charged AOT-AuNPs show specific adsorption to Pt surfaces. In the same buffer, the MOA-capped AuNPs selectively bind to Pt surfaces in the protonated state at pH 9, while they bind preferably to AuPd surfaces in mild acidic conditions at pH 5 (Figure 6).[24b]

Besides this, adsorption properties can be adjusted by adding specific electrolytes, following the Hofmeister series. In par-

Minireview
doi.org/10.1002/ejic.202000629

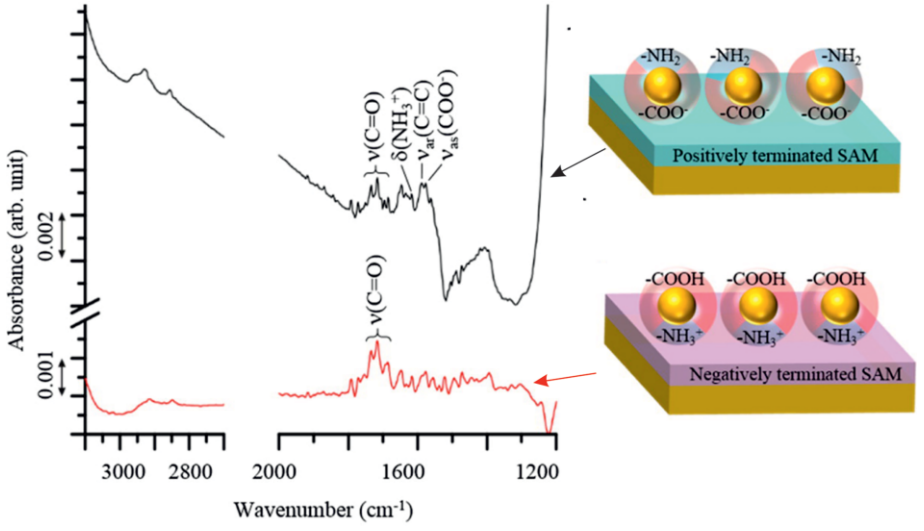

Figure 5. Directed self-assembly of Janus-AuNP and detection with IRRAS. Adapted with permission from ref.[4b] Copyright (2016) American Chemical Society.

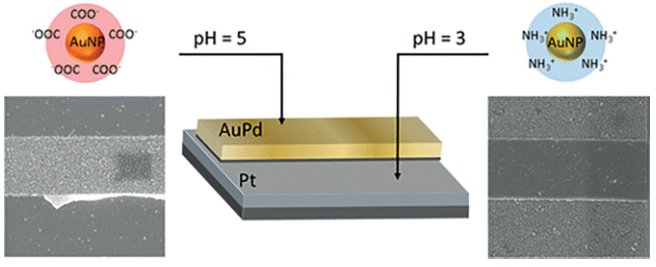

Figure 6. Differential adsorption on Pt and AuPd of AuNP capped with amine and carboxylic acid terminated ligands.[24b] Reprinted with permission from ref.[24b] Copyright (2014) American Chemical Society.

ticular, metal chlorides (MCl, M^+ = Li^+, Na^+, K^+, Cs^+) have an effect on the adsorption of AOT and MOA AuNP on Pt and AuPd surfaces. Both types of AuNP indicate a primary adsorption on Pt, while the highest adsorption can be obtained with Li^+.[21c]

3. Nano-Gapped Electrodes for Molecular Electronic Devices

In the last decade, multiple routes to fabricate nano-gapped electrodes have been developed that allow for the formation of purpose-built metal-molecule-metal structures. These experimental platforms enable the in-depth study of the metal-molecule contact or the physical properties of single molecules and, thus, are substantial for the development of molecular devices.[53] However, it is essential for the integration capability of molecular electronics that the fabrication method of nanoelectrodes is compatible to the state-of-the-art optical lithographic methods used for patterning CMOS devices. Furthermore, there is the need to fabricate nanoelectrodes with high yield and sub-nanometer precision to enable reproducible molecular electronic devices.[54] These requirements are best met by electron beam lithography (EBL). In EBL, nanostructures are created by patterning a resist layer with a focused beam of electrons. The high energetic electrons alter the solubility of the exposed resist, which can subsequently be removed selectively by a developer.[55] Present-day EBL systems, with 100 kV accelerator voltage or more, together with appropriate e-beam resists enable fine patterns with up to 10 nm resolution. Even higher resolutions can be realized in research settings using thoroughly controlled e-beam writers with a beam diameter of about 3 nm and a correction of the EBL inherent proximity effect.[56] The proximity effect leads to the reduction of the resolution due to the lateral scattering of secondary electrons from the exposed area in resist and substrate. Employing specialized design correction software the proximity error can be reduced to a large extent.[55]

While it is possible to directly fabricate homometallic nanoelectrodes with a sub-10 nm separation using EBL in a lift-off process,[56] heterometallic nanoelectrodes need more sophisticated approaches that allow to introduce an asymmetry into a molecular device. Heterometallic nanoelectrodes can be produced by two subsequent EBL and lift-off processes with the need of a precise alignment, by electrodeposition of a second metal on one nanoelectrode,[57] or by applying a self-alignment procedure combined with EBL.[58] Recently, we succeeded in fabricating heterometallic nanoelectrode pairs with a separation of 10 ± 3 nm and a yield of over 60 % using EBL in a lift-off process in combination with the Al_2O_3 hard mask.[21b,24c] This method allows to adjust the size of the gap between the electrodes in the nanometer scale by the thickness of the Al_2O_3 layer. Using self-alignment of the electrodes based on an Al_2O_3 hard mask is a method to reliably produce nanometer-sized gaps independent of alignment risks during several involved lithography steps (Figure 7). These advances in the fabrication of nanometer-sized electrode structures by EBL and lift-off enable devices based on only one single molecularly functionalized AuNP.

Minireview
doi.org/10.1002/ejic.202000629

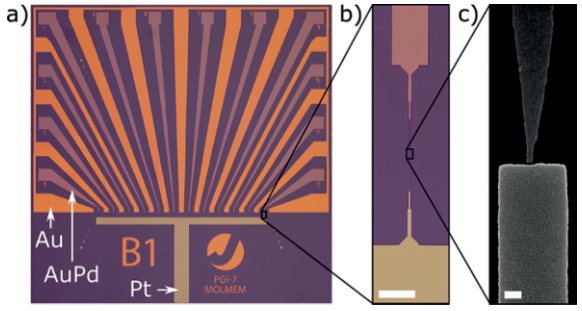

Figure 7. Sample design. (a) Optical microscope image of a 6 × 6 mm² SiO_2/Si sample with 12 nanoelectrode gaps located between AuPd-electrodes (pink) and one common T-shaped Pt-electrode (ochre). The AuPd-electrodes are surrounded by an Au-shield (orange). (b) Close-up of one electrode pair (scale bar = 20 µm). (c) SEM image of one electrode pair with a gap of 10 nm (scale bar = 100 nm).[24c] Reprinted with permission from ref.[24c] Copyright (2019) American Chemical Society.

4. Molecular Electronic Devices Based on Ordered AuNP Arrays

2D nanoparticle arrays can be produced by different methods, like the Langmuir–Blodgett (LB) technique, drying-mediated assembly on a solid substrate (drop-drying) or on a water surface,[59] and the aforementioned SAM-mediated assembly.[47] Using the LB method, first a drop of the nanoparticle suspension is deposited onto a water surface in a LB trough. Then, the resulting AuNP film is compressed by a movable barrier until a desired particle density is reached. Subsequently, the formed nanoparticle monolayer is transferred, for example by microcontact printing, onto an arbitrary substrate. This method allows to control the packing density and the particle organization of the AuNP assembly and is well-suited to obtain reproducible, highly ordered 2D arrays. However, the facile drying-mediated assembly is often used, since it provides a low-cost approach towards close-packed AuNP arrays.

As already described, AuNPs are stabilized by organic surfactants to prevent aggregation during the synthesis and to ensure colloidal stability as well as solubility. Frequently used stabilizing ligands are alkanethiols because they are able to form the stable Au–S chemical bonds on the AuNP side and lead to highly ordered AuNP arrays due to interdigitating of the alkane chains of neighboring NPs, which is triggered by intermolecular van der Waals forces. Furthermore, the length of the alkane chains can be adapted to define the interparticle distance. Consequently, 2D assemblies of alkanethiol-capped AuNPs between electrode structures can be regarded as test devices for molecular components.[59a,60] Molecules of interest can be incorporated into the AuNP arrays by immersing the AuNPs device into a solution of these molecules. Especially favorable is to use long chain, conjugated molecules or molecules with a certain functionality equipped with thiol groups at both ends to exchange the alkanethiol ligands. The two thiol end groups offer the possibility to interconnect AuNPs and thus, result in a network of AuNPs with increased conductivity and/or functionality. Using this procedure it is possible to realize switching devices, triggered by an electrical field, UV/Visible light or plasmon-induced resonance energy transfer,[13a,61] or devices with the ability of chemical and mechanical sensing.[59a,60]

Interestingly, in order to approach molecular scale electronic devices, a light-switchable, planar nanodevice with a large on/off ratio based on isotropically functionalized AuNP was reported.[61b] The device is formed by a self-assembled nanoparticle network that is contacted by nanoelectrodes with a separation of 30 to 100 nm. The employed 10 nm AuNP are functionalized with azobenzene-bithiophene molecules which are known to exhibit *cis*/*trans* isomerization under irradiation by visible light at different wavelengths. Thus, a reversibly switching device with an average on/off ratio of 30 is obtained based on the conformational switching of an azobenzene derivative between a high conductive *cis* configuration and a low conductive *trans* configuration (Figure 8).

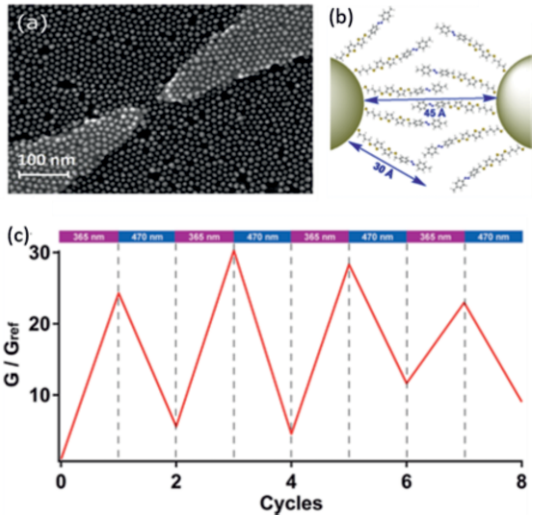

Figure 8. (a) SEM image showing the azobenzene-bithiophene AuNP network. (b) Schematic of the interdigitation between molecules from adjacent AuNP. (c) Plot of normalized conductance (G/G_{ref}) showing light-induced switching of the device. Reprinted with permission from ref.[61b] Copyright (2015) American Chemical Society.

A completely different concept to establish electronic circuits is based on AuNPs homogeneously covered with charged ligands.[62] While layers of AuNPs capped with 11-mercaptoundecanoic acid show linear current-voltage characteristics under bias and can be used as resistors, two laminated layers of oppositely charged AuNPs exhibit diode characteristics. The underlying concept is that the small counterions that surround the AuNPs interdiffuse at the interface of the two AuNP layers and thus form an internal electric field. The interdiffusion is entropically driven. If an external field is applied, the resulting current through the device will show different values depending on the direction of the applied field (Figure 9). Besides these rectifying bilayers, also sensing AuNP layers are possible, if the conduction properties of the capping ligands are influenced by adsorbed molecules, like H_2O, CO_2, or other gases.[62,63]

5. Towards Single AuNP Devices

In order to achieve the next step of miniaturization, we aim to bridge sub-10 nm gaps between two nanoelectrodes by only

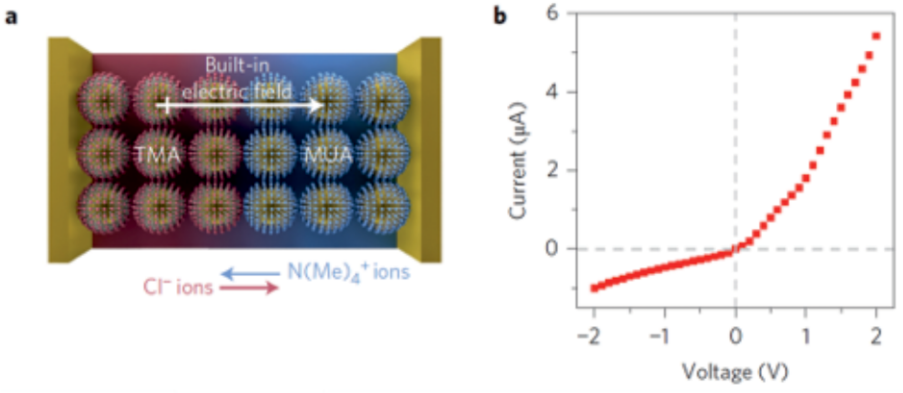

Figure 9. Electrical characteristics of metal nanoparticle diodes: (a) Scheme of the bilayer diode, (b) current-voltage characteristics for the bilayer device. Reprinted by permission from ref.[62] Copyright Springer Nature (2016).

one single molecularly functionalized AuNP.[64] An AuNP can be immobilized in the nanogap by the drop-drying method or by the more directed but more elaborate method dielectrophoresis.[65] When using dielectrophoresis, an inhomogeneous electrical field based on a combination of a direct and an alternating current (AC and DC) is applied in order to direct the AuNP into the region of high electric field strength – that is, into the gap between the nanoelectrodes. Usually, a DC ramp combined with an AC signal with a fixed frequency is used, while a drop of a very dilute suspension of the respective AuNPs is covering the nanoelectrodes. Furthermore, a reference resistor with a resistance in the range of the nanoparticle device needs to be connected in series (Figure 10). Then the trapping of a nanoparticle between the nanoelectrodes causes a variation of the AC signal over the reference resistor, which can be measured with a lock-in amplifier. At the same time, the resistance of the AuNP device is reduced considerably, so that the main part of the voltage drops over the reference resistor precluding a second trapping event.[64,65] Thus, dielectrophoresis offers an elegant method to immobilize only one AuNP in a nanogap. However, difficulties may appear, if the AuNP solvent has a high evaporation rate or if charged particles should be trapped.

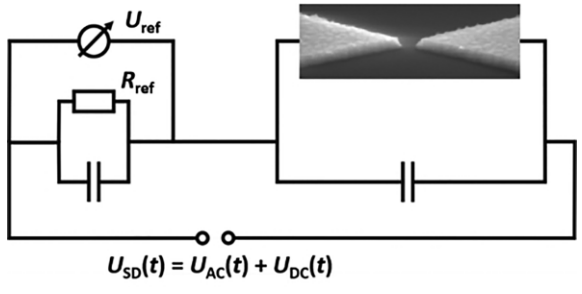

Figure 10. Schematic of an equivalent circuit of the trapping equipment with the applied voltage $U(t) = U_{AC}(t) + U_{DC}(t)$, the reference resistor R_{ref}, and the stray capacity C_{stray} together with the SEM image of a nanogap.[65]

Single AuNP devices in the sub-10 nm regime were achieved by dielectrophoretic trapping of biphenylpropanethiol (BP) capped AuNPs with a core diameter of 4.1 ± 0.5 nm in gaps formed by homometallic nanoelectrodes (gap size 5 ± 1 nm) in a CMOS-adapted device geometry.[64,65] The thickness of the ligand shell including solvent molecules was determined by DLS and SAXS measurements to be approximately 0.8 nm. Thus, the size of the nanogap was adequately adapted to the size of the BP-AuNP, which is a prerequisite for a functional device. A possible vacuum gap between nanoparticle and electrode of only 0.1 nm would reduce the conductance through the device by a factor of 10. Moreover, slight changes in the contact geometry, like a displacement of single metal atoms, an expansion/contraction of the nanoelectrodes due to variations in temperature, structural transitions of nanoparticles, or changes in the configuration of the molecules, would lead to significant, irreversible changes in transport characteristics of single AuNP devices. It is all the more astonishing that the formed BP-AuNP devices were stable for several weeks in a cryostat under inert gas atmosphere.

Possible transport mechanisms in arrays of AuNPs and in single AuNP devices forming "nanoelectrode-molecule/AuNP/molecule-nanoelectrode" junctions include:

(i) thermally activated electron hopping between nearest neighbors following the Arrhenius relation ($\ln G \approx 1/T$, with G = conductance and T = temperature),

(ii) superexchange coupling between next nearest neighbors exhibiting a considerably weaker temperature dependence [$\ln(G \times T^{0.5}) \approx 1/T$], and

(iii) electron tunneling through very thin barriers without significant temperature dependence. If high electric fields are applied

(iv) thermionic emission can be discussed for electron transport in molecular devices as well, accompanied by a strong temperature dependence [$\ln(G/T^2) \approx 1/T$].

Accordingly, investigations of the temperature dependence of the conductance are suitable means to identify the predominant electron transport mechanisms. In the case of BP-AuNP four different transport regimes could be attributed to different transport mechanisms, Figure 11.[64] Moreover, the single BP-AuNP device showed Coulomb blockade behavior at 4 K and at room temperature.

Impressive examples that the molecule-electrode contact distinctly determines the transport properties are single AuNP devices based on MPA-AuNP and MPTP-AuNP.[21b,24c] In both cases the degree of protonation of the ligand shell influences

Minireview
doi.org/10.1002/ejic.202000629

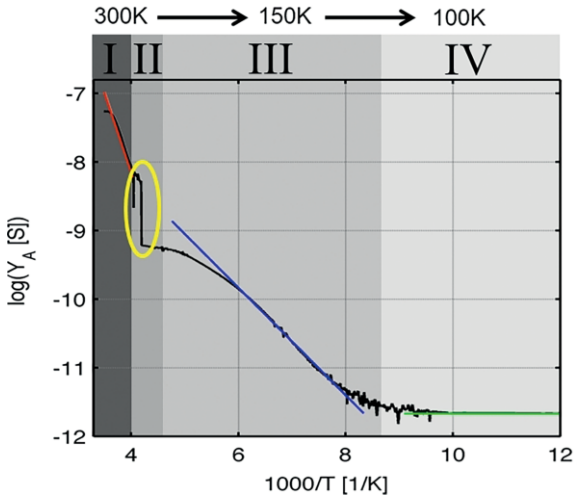

Figure 11. Conductance (Y_A) of a single BP-AuNP device plotted as log(Y_A) vs. 1/T. Four different transport regimes can be identified according to their temperature dependence: (i) thermally activated hopping, (ii) significant singularity in conductance (structural phase transition in AuNP core), (iii) super-exchange coupling, (iv) tunneling regime.[64] Adapted with permission from ref.[64] Copyright (2012) American Chemical Society.

the formation of the molecule-metal interface. In case of MPA-AuNP, water molecules incorporated into the ligand shell and involved in hydrogen bonds to the terminal amine groups of MPA were identified by XPS measurements.[21b] This additional water shell leads to a considerably reduced device conductance due to the increased shell size and reduced MPA-metal coupling. Even more possibilities to form different molecule-metal contacts are offered by a terminal terpyridine group (TP), like given in MPTP-AuNPs. Here, depending on the protonation of TP, a contact to the electrode is formed by one or two outer pyridine moieties or by the whole TP (Figure 12).[24c] Only a treatment of the MPTP-AuNP device by an ammonia solution enables the removal of protons ligated to the terminal TP resulting in a robust TP-electrode contact and a short tunneling distance through MPTP. These findings indicate that it is mandatory to control the chemical environment of functionalized AuNPs in order to obtain the desired molecule-metal contacts and envisaged device functionalities.

So far, we have shown that single, molecularly functionalized AuNPs are suited as building blocks for sub-10 nm nanoscale devices. However, a formidable step in miniaturization would be achieved, if these AuNP devices exhibited an intrinsic asymmetry, like required for rectification. Based on our work on transport through molecular devices and the preferred formation of distinct molecule-electrode contacts, we developed a concept for a rectifying AuNP device.[24a,24b,35] This prototypical device should be achieved by utilizing heterometallic electrodes and corresponding Janus-type AuNP with adequately chosen ligands. The Janus-AuNP were stabilized by MOA and MPA on opposite hemispheres. The heterometallic nanogaps were formed by Pt and AuPd electrodes and the size was adjusted to the size of the Janus-AuNP (Figure 13). Thus, the preferred molecular anchor group-metal combination, N-Pt, could be used to immobilize the Janus-AuNP in a directed way by dielectrophoretic trapping and the COO-AuPd bond could be

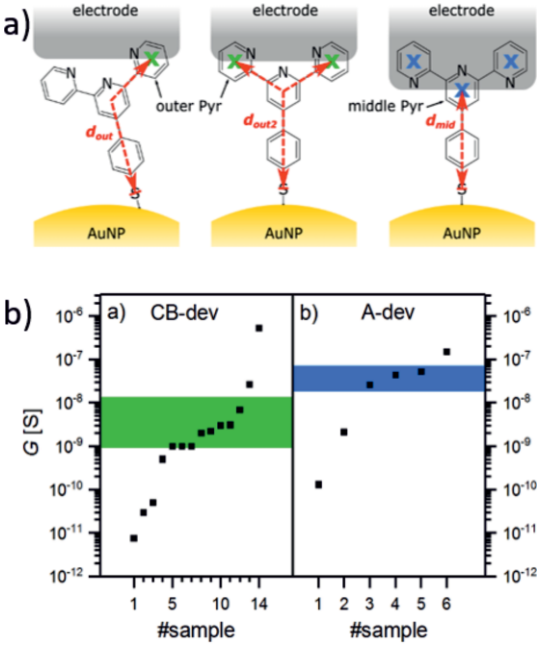

Figure 12. (a) Schematic displaying possible contact configurations at the terpyridine-electrode interface and the resulting tunneling path. (b) Conductance values of single MPTP-AuNP devices in ascending order. CB-devices (treated with carbonate buffer) exhibit conductance values corresponding to electrode contacts with one or two outer pyridine groups (green), while A-devices (treated with ammonia solution) show larger conductance values corresponding to a strong terpyridine-electrode contact (blue).[24c] Adapted with permission from ref.[24c] Copyright (2019) American Chemical Society.

formed at the counter electrode. The resulting devices, Pt-MPA/AuNP/MOA-AuPd, were identified to form asymmetric double-barrier tunneling junctions. The determined current-voltage curves exhibit a distinct asymmetry in the voltage range 0.3 V to 0.8 V (see red double arrows in Figure 13) which can be attributed to the different tunneling barriers corresponding to tunneling junctions formed by MPA and MOA on the opposite hemispheres of the AuNP. This could be verified by a thorough analysis of the adsorption behavior of the Janus-AuNP by XPS. Additionally, an estimation of the device conductance was performed on basis of the single channel Landauer formula assuming only one tunneling path through one molecule on each

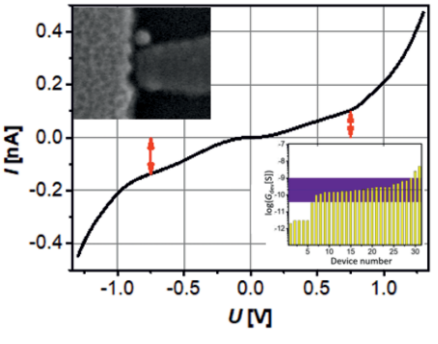

Figure 13. I/U measurement with an asymmetric slope. Insets: SEM image of the Janus-AuNP device (left) and statistics of experimental conductance values of 37 devices at U_{SD} = 1 V (right).[24a] Adapted with permission from ref.[24a] Copyright (2014) American Chemical Society.

side of the AuNP, respectively. In principle, a few molecules could contribute to the device conductance, but the number is very limited due to the curvature of the AuNP and the exponential dependence of the conductance on the tunneling distance as mentioned above. However, it turned out that estimated conductance values, obtained by applying the single channel Landauer formula, the decay constants and tunneling distances determined by the respective molecule as well as the appropriate transmission coefficients characterizing the respective molecule-metal contacts, are in good agreement with the experimentally obtained device conductances. The statistics of the measured conductance values (Figure 13) demonstrates the high reproducibility of these devices formed by directed assembly of Janus-AuNP in heterometallic nanogaps. In view of the huge variation in conductance by just very slight variations in vacuo gap site, these data already reflect a high reproducibility and lift the results already beyond a single proof-of-concept.

Next, we investigated the transport behavior of AuNP functionalized with RuMPTP complexes.[24d] Ru-MPTP complexes are electrofunctional molecules with an intrinsic switching ability which is accompanied only by small configurational changes. Remarkably, distinct hysteretic current vs. voltage characteristics can be obtained also from single RuMPTP-AuNP in device geometry. In Figure 14, representative hysteresis curves are given for two kinds of obtained devices, with high and low conductance, respectively. The maximum on/off ratio of 1.5, determined for both kinds of devices, is in line with values of 1.07 and 3 given for monolayer-based molecular devices employing Ru-MPTP complexes as switching elements.[24d,66] The *I*/*U*-curve of the high conductance device exhibits a symmetric transport characteristic as expected for a symmetric device. However, the *I*/*U*-curve given in Figure 14 (b) is asymmetric. One likely explanation for this is an asymmetric double-barrier tunnel junction, which results from an incomplete hydrolysis of a part of the thiol protecting acetyl groups during immobilization. The thus built asymmetric contacts at the MPTP-electrode interfaces directly affect the transport behavior through the two tunnel junctions on both sides of the AuNP. This indicates that, asymmetric double-barrier tunnel junctions built by incomplete hydrolysis of thiol protecting groups can introduce a rectifying character. The hysteretic transport characteristic (Figure 14) denotes that single RuMPTP-AuNP devices based on voltage-driven switching transition metal complexes can be integrated in CMOS compatible devices to form storage elements.

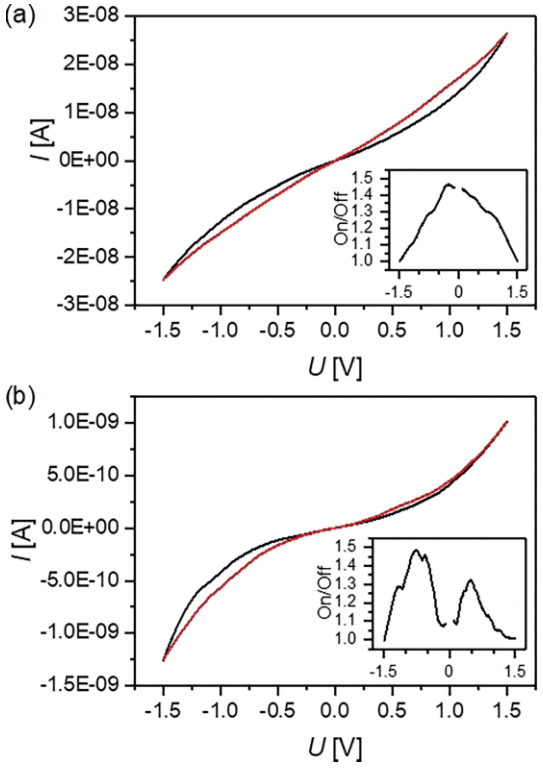

Figure 14. Hysteretic current vs. voltage characteristics of a RuMPTP-AuNP device, ascending (red) and descending (black) *I*/*U*-curves (a) high conductance device, (b) low conductance device. Insets: on/off ratio in each case.[24d] Reprinted with permission from ref.[24d] Copyright (2020) American Chemical Society.

6. Summary and Conclusion

In the past decade, the concept of building up nanoelectronic devices based on chemically tailored metal NPs has evolved from initially utilizing the Coulomb charging energy to build up single electron devices. At present, the field moves to a higher level of integration, where new functionalities are being explored that are introduced by the stabilizing ligands. This requires a high degree of control of the particle functionalization, the ligand-electrode interface which allows for directed integration, as well as of the nanoelectrode fabrication process on the sub-10 nm level.

In this minireview, we strived for acquainting the reader with the progress in the field by summarizing examples, predominantly taken from our most recent work. Based on the present day of knowledge, we assume that following the concept of integrating molecular electronic devices into traditional CMOS circuitry, hybrid nanoelements, like molecularly functionalized metal nanoparticles as discussed here, can be advantageously employed to enable additional functionality. However, one of the big challenges in setting up such devices is to control exactly the electronic function of the molecule-metal junction by design. As a first step in this direction, we introduced divalent bifunctional (Janus-type) AuNPs integrated into a heterometallic nano-gap. Thereby a diode function is realized due to the assembly of a single Janus particle in a directed manner. We would like to point out that alternative concepts are being explored as well, such as the integration of so-called "protodevices", i.e. AuNP pairs linked by a single of few molecules, into prefabricated electrodes utilizing surface charge interactions,[67] or by combinations of AuNPs and gold nanorods, bridging the gap between nano- and microscale,[68] however, in a non-directional manner.

Further progress is achieved when molecules acting as molecular switches are applied to stabilize and integrate the AuNPs. Such molecules imply intrinsic switching functionalities which can be addressed by optical[69] or electrical means.[70] In future, Janus-type AuNPs functionalized by combinations of molecular rectifiers and switches will be obtained. This would

allow for building up higher integrated circuits, such as crossbar architectures, which require both electrical functionalities to avoid cross talk and enable memory functionality. This may be a great opportunity for a general new type of electronic devices. However, such effects have not been studied experimentally or theoretically in much detail yet. The presently applied computational models are at least incomplete with respect to the huge variety of the different control parameters in nanodevices formed by molecularly functionalized metal NPs.

In essence, the complex interplay of particle size and size distribution, constitution, symmetry and conformation of the ligand molecules, of the state of charge of the particles, of the embedding media and dielectric environment is not yet understood well enough. Furthermore, it is not foreseeable how stable NPs and the respective molecular objects will be under the operating conditions of a high performance electrical circuit. Answering these questions will undoubtedly be one of the great challenges in nanomaterials chemistry.

Acknowledgments

The authors are grateful to the German Research Foundation for financial support of several projects on this topic, which also enabled the funding of, inter alia, S. P.'s Ph.D. endeavor. We furthermore thank Thomas Poessinger for technical assistance in figure preparation and Greta Haselmann for proofreading of the manuscript. U. S. appreciates generous financial support by the Excellence Initiative of the German federal and state governments to promote science and research at German universities. Open access funding enabled and organized by Projekt DEAL.

Keywords: Gold · Nanoparticles · Nanoelectrodes · Molecular wires · Janus particles · Nanoelectronics

[1] a) N. Khlebtsov, L. Dykman, *Chem. Soc. Rev.* **2011**, *40*, 1647–1671; b) M. Homberger, U. Simon, *Philos. Trans. R. Soc. London Ser. A* **2010**, *368*, 1405–1453; c) N. Li, P. Zhao, D. Astruc, *Angew. Chem. Int. Ed.* **2014**, *53*, 1756–1789; *Angew. Chem.* **2014**, *126*, 1784; d) V. Amendola, R. Pilot, M. Frasconi, O. M. Maragò, M. A. Iatì, *J. Phys. Condens. Matter* **2017**, *29*, 203002; e) L. Qin, G. Zeng, C. Lai, D. Huang, P. Xu, C. Zhang, M. Cheng, X. Liu, S. Liu, B. Li, H. Yi, *Coord. Chem. Rev.* **2018**, *359*, 1–31.

[2] J. R. Reimers, M. J. Ford, S. M. Marcuccio, J. Ulstrup, N. S. Hush, *Nat. Rev. Chem.* **2017**, *1*, 0017.

[3] J. P. Hermes, F. Sander, U. Fluch, T. Peterle, D. Thompson, R. Urbani, T. Pfohl, M. Mayor, *J. Am. Chem. Soc.* **2012**, *134*, 14674–14677.

[4] a) H. Kim, R. P. Carney, J. Reguera, Q. K. Ong, X. Liu, F. Stellacci, *Adv. Mater.* **2012**, *24*, 3857–3863; b) S. D. M. Bourone, C. Kaulen, M. Homberger, U. Simon, *Langmuir* **2016**, *32*, 954–962.

[5] a) G. Schmid, G. Schön, U. Simon, USA Patent No. 08/041, 239, **1992**; b) U. Simon, G. Schön, G. Schmid, *Angew. Chem. Int. Ed. Engl.* **1993**, *32*, 250–254; *Angew. Chem.* **1993**, *105*, 264; c) G. Schmid, *Chem. Rev.* **1992**, *92*, 1709–1727; d) D. L. Feldheim, C. D. Keating, *Chem. Soc. Rev.* **1998**, *27*, 1–12.

[6] A. Taleb, F. Silly, A. O. Gusev, F. Charra, M.-P. Pileni, *Adv. Mater.* **2000**, *12*, 633–637.

[7] L. J. de Jongh, *Physics and Chemistry of Metal Cluster Compounds*, Kluwer Academic Publishers, Dordrecht **1994**.

[8] A. J. Quinn, M. Biancardo, L. Floyd, M. Belloni, P. R. Ashton, J. A. Preece, C. A. Bignozzi, G. Redmond, *J. Mater. Chem.* **2005**, *15*, 4403–4407.

[9] W. J. Parak, L. Manna, F. C. Simmel, D. Gerion, P. Alivisatos, Quatum Dots in *Nanoparticles*: *From theory to Application* (Ed.: G. Schmid), **2010**, Wiley–VCH, **2010**, pp. 3–47.

[10] T. Sato, H. Ahmed, *Appl. Phys. Lett.* **1997**, *70*, 2759–2761.

[11] Y. Majima, G. Hackenberger, Y. Azuma, S. Kano, K. Matsuzaki, T. Susaki, M. Sakamoto, T. Teranishi, *Sci. Technol. Adv. Mater.* **2017**, *18*, 374–380.

[12] a) S. Jan van der Molen, P. Liljeroth, *J. Phys. Condens. Matter* **2010**, *22*, 133001; b) M. Kiguchi, S. Kaneko, *ChemPhysChem* **2012**, *13*, 1116–1126.

[13] a) J. Liao, M. A. Mangold, S. Grunder, M. Mayor, C. Schönenberger, M. Calame, *New J. Phys.* **2008**, *10*, 065019; b) N. Olichwer, A. Meyer, M. Yesilmen, T. Vossmeyer, *J. Mater. Chem. C* **2016**, *4*, 8214–8225.

[14] a) H. Schlicke, M. Rebber, S. Kunze, T. Vossmeyer, *Nanoscale* **2016**, *8*, 183–186; b) N. Olichwer, E. W. Leib, A. H. Halfar, A. Petrov, T. Vossmeyer, *ACS Appl. Mater. Interfaces* **2012**, *4*, 6151–6161.

[15] J. Trasobares, D. Vuillaume, D. Théron, N. Clément, *Nat. Commun.* **2016**, *7*, 12850.

[16] A. Vahl, N. Carstens, T. Strunskus, F. Faupel, A. Hassanien, *Sci. Rep.* **2019**, *9*, 17367.

[17] a) S. Jan van der Molen, E. S. R. Naaman, A. N. J. Neaton, D. Natelson, N. Tao, H. v. d. Zant, M. Mayor, M. Ruben, M. Reed, M. Calame, *Nat. Nanotechnol.* **2013**, *8*, 385–389; b) G. M. Whitesides, *Annu. Rev. Anal. Chem.* **2013**, *6*, 1–29; c) E. Lortscher, *Nat. Nanotechnol.* **2013**, *8*, 381–384; d) Y. Ji, D. F. Zeigler, D. S. Lee, H. Choi, A. K. Y. Jen, H. C. Ko, T.-W. Kim, *Nat. Commun.* **2013**, *4*, 2707.

[18] a) M.-C. Daniel, D. Astruc, *Chem. Rev.* **2004**, *104*, 293–346; b) J. Zhou, J. Ralston, R. Sedev, D. A. Beattie, *J. Colloid Interface Sci.* **2009**, *331*, 251–262; c) G. Schmid, U. Simon, *Chem. Commun.* **2005**, 697–710.

[19] a) G. Frens, *Nat. Phys. Sci.* **1973**, *241*, 20–22; b) J. Turkevich, P. C. Stevenson, J. Hillier, *Discuss. Faraday Soc.* **1951**, *11*, 55–75; c) M. Wuithschick, A. Birnbaum, S. Witte, M. Sztucki, U. Vainio, N. Pinna, K. Rademann, F. Emmerling, R. Kraehnert, J. Polte, *ACS Nano* **2015**, *9*, 7052–7071; d) J. C. Love, L. A. Estroff, J. K. Kriebel, R. G. Nuzzo, G. M. Whitesides, *Chem. Rev.* **2005**, *105*, 1103–1170.

[20] J. Polte, *CrystEngComm* **2015**, *17*, 6809–6830.

[21] a) F. Chen, X. Li, J. Hihath, Z. Huang, N. Tao, *J. Am. Chem. Soc.* **2006**, *128*, 15874–15881; b) N. Babajani, P. Kowalzik, R. Waser, M. Homberger, C. Kaulen, U. Simon, S. Karthäuser, *J. Phys. Chem. C* **2013**, *117*, 22002–22009; c) C. Kaulen, U. Simon, *RSC Adv.* **2018**, *8*, 1717–1724; d) R. Liffmann, M. Homberger, M. Mennicken, S. Karthäuser, U. Simon, *RSC Adv.* **2015**, *5*, 102981–102992; e) T. C. Preston, M. Nuruzzaman, N. D. Jones, S. Mittler, *J. Phys. Chem. C* **2009**, *113*, 14236–14244.

[22] a) K. D. Collins, *Methods* **2004**, *34*, 300–311; b) F. Hofmeister, *Archiv für experimentelle Pathologie und Pharmakologie* **1888**, *24*, 247–260.

[23] a) M. G. Bellino, E. J. Calvo, G. Gordillo, *Phys. Chem. Chem. Phys.* **2004**, *6*, 424–428; b) N. Chauhan, S. Gupta, N. Singh, S. Singh, S. S. Islam, K. N. Sood, R. Pasricha, *J. Colloid Interface Sci.* **2011**, *363*, 42–50; c) D. A. Giljohann, D. S. Seferos, W. L. Daniel, M. D. Massich, P. C. Patel, C. A. Mirkin, *Angew. Chem. Int. Ed.* **2010**, *49*, 3280–3294; *Angew. Chem.* **2010**, *122*, 3352.

[24] a) N. Babajani, C. Kaulen, M. Homberger, M. Mennicken, R. Waser, U. Simon, S. Karthäuser, *J. Phys. Chem. C* **2014**, *118*, 27142–27149; b) C. Kaulen, M. Homberger, S. Bourone, N. Babajani, S. Karthäuser, A. Besmehn, U. Simon, *Langmuir* **2014**, *30*, 574–583; c) M. Mennicken, S. K. Peter, C. Kaulen, U. Simon, S. Karthäuser, *J. Phys. Chem. C* **2019**, *123*, 21367–21375; d) M. Mennicken, S. K. Peter, C. Kaulen, U. Simon, S. Karthäuser, *J. Phys. Chem. C* **2020**, *124*, 4881–4889.

[25] a) X. Han, Y. Li, S. Wu, Z. Deng, *Small* **2008**, *4*, 326–329; b) C.-w. Lee, C. Takagi, T. Truong, Y.-C. Chen, A. Ostafin, *J. Phys. Chem. C* **2010**, *114*, 12459–12468.

[26] N. Nath, A. Chilkoti, *Anal. Chem.* **2004**, *76*, 5370–5378.

[27] A. Üzer, Z. Can, İ. Akın, E. Erçağ, R. Apak, *Anal. Chem.* **2014**, *86*, 351–356.

[28] Y. Song, S. Chen, *Chem. Asian J.* **2014**, *9*, 418–430.

[29] D. J. Cole-Hamilton, *Science* **2010**, *327*, 41–42.

[30] N. Glaser, D. J. Adams, A. Böker, G. Krausch, *Langmuir* **2006**, *22*, 5227–5229.

[31] F. Sciortino, A. Giacometti, G. Pastore, *Phys. Rev. Lett.* **2009**, *103*, 237801.

[32] a) F. Ciesa, A. Plech, *J. Colloid Interface Sci.* **2010**, *346*, 1–7; b) D. M. Andala, S. H. R. Shin, H.-Y. Lee, K. J. M. Bishop, *ACS Nano* **2012**, *6*, 1044–1050.

[33] R. Sardar, T. B. Heap, J. S. Shumaker-Parry, *J. Am. Chem. Soc.* **2007**, *129*, 5356–5357.
[34] N. Babajani, Doktorarbeit thesis, (RWTH Aachen University), **2014**.
[35] S. Karthäuser, *J. Phys. Condens. Matter* **2011**, *23*, 013001.
[36] D. Bartczak, A. G. Kanaras, *Langmuir* **2010**, *26*, 7072–7077.
[37] a) Y. Song, L. M. Klivansky, Y. Liu, S. Chen, *Langmuir* **2011**, *27*, 14581–14588; b) H. Menzel, M. D. Mowery, M. Cai, C. E. Evans, *Macromol. Symp.* **1999**, *142*, 23–31.
[38] A. Winter, M. D. Hager, G. R. Newkome, U. S. Schubert, *Adv. Mater.* **2011**, *23*, 5728–5748.
[39] a) A. Duerrbeck, S. Gorelik, J. Hobley, A. M. Yong, G. S. Subramanian, A. Hor, N. Long, *J. Mater. Chem. C* **2015**, *3*, 8992–9002; b) F.-S. Han, M. Higuchi, D. G. Kurth, *Tetrahedron* **2008**, *64*, 9108–9116; c) A. Wild, A. Winter, F. Schlütter, U. S. Schubert, *Chem. Soc. Rev.* **2011**, *40*, 1459–1511; d) U. S. Schubert, H. Hofmeier, G. R. Newkome, in *Modern Terpyridine Chemistry*, WILEY-VCH Verlag GmbH & Co. KGaA, Weinheim, **2006**, pp. 37–68; e) U. S. Schubert, H. Hofmeier, G. R. Newkome, in *Modern Terpyridine Chemistry*, WILEY-VCH Verlag GmbH & Co. KGaA, Weinheim, **2006**, pp. 69–130; f) U. S. Schubert, H. Hofmeier, G. R. Newkome, in *Modern Terpyridine Chemistry*, WILEY-VCH Verlag GmbH & Co. KGaA, Weinheim, **2006**, pp. 199–218; g) E. C. Constable, *Chem. Soc. Rev.* **2007**, *36*, 246–253; h) E. C. Constable, M. Devereux, E. L. Dunphy, C. E. Housecroft, J. A. Rudd, J. A. Zampese, *Dalton Trans.* **2011**, *40*, 5505–5515; i) E. C. Constable, C. E. Housecroft, E. Medlycott, M. Neuburger, F. Reinders, S. Reymann, S. Schaffner, *Inorg. Chem. Commun.* **2008**, *11*, 518–520; j) E. C. Constable, A. M. W. C. Thompson, *J. Chem. Soc., Dalton Trans.* **1992**, 3467–3475; k) T.-Y. Dong, C. Huang, C.-P. Chen, M.-C. Lin, *J. Organomet. Chem.* **2007**, *692*, 5147–5155.
[40] a) A. G. Majouga, R. B. Romashkina, A. S. Kashaev, R. D. Rahimov, E. K. Beloglazkina, N. V. Zyk, *Chem. Heterocycl. Compd.* **2010**, *46*, 1076–1083; b) M. Montalti, L. Prodi, N. Zaccheroni, M. Beltrame, T. Morotti, S. Quici, *New J. Chem.* **2007**, *31*, 102–108; c) M. Ito, T. Tsukatani, H. Fujihara, *J. Mater. Chem.* **2005**, *15*, 960–964.
[41] A. Auditore, N. Tuccitto, G. Marzanni, S. Quici, F. Puntoriero, S. Campagna, A. Licciardello, *Chem. Commun.* **2003**, 2494–2495.
[42] K. Nakamoto, *J. Phys. Chem.* **1960**, *64*, 1420–1425.
[43] N. Tuccitto, V. Torrisi, M. Cavazzini, T. Morotti, F. Puntoriero, S. Quici, S. Campagna, A. Licciardello, *ChemPhysChem* **2007**, *8*, 227–230.
[44] T.-Y. Dong, H.-W. Shih, L.-S. Chang, *Langmuir* **2004**, *20*, 9340–9347.
[45] D. Rajarathnam, J. Babu, P. A. Nadar, *Int. J. Chem. Kinet.* **2002**, *34*, 18–26.
[46] J. C. Huie, *Smart Mater. Struct.* **2003**, *12*, 264–271.
[47] a) T. Zhu, X. Fu, T. Mu, J. Wang, Z. Liu, *Langmuir* **1999**, *15*, 5197–5199; b) T. Okamoto, I. Yamaguchi, *J. Phys. Chem. B* **2003**, *107*, 10321–10324; c) G. Chumanov, K. Sokolov, B. W. Gregory, T. M. Cotton, *J. Phys. Chem.* **1995**, *99*, 9466–9471.
[48] a) S. Huang, G. Tsutsui, H. Sakaue, S. Shingubara, T. Takahagi, *J. Vac. Sci. Technol. B* **2001**, *19*, 2045–2049; b) J. J. Brown, J. A. Porter, C. P. Daghlian, U. J. Gibson, *Langmuir* **2001**, *17*, 7966–7969.
[49] a) M. Brust, D. Bethell, C. J. Kiely, D. J. Schiffrin, *Langmuir* **1998**, *14*, 5425–5429; b) H. Fan, G. P. López, *Langmuir* **1997**, *13*, 119–121.
[50] a) S. Gilles, C. Kaulen, M. Pabst, U. Simon, A. Offenhäusser, D. Mayer, *Nanotechnology* **2011**, *22*, 295301; b) Y. Ofir, B. Samanta, V. M. Rotello, *Chem. Soc. Rev.* **2008**, *37*, 1814–1825.
[51] C. Vericat, M. E. Vela, G. Benitez, P. Carro, R. C. Salvarezza, *Chem. Soc. Rev.* **2010**, *39*, 1805–1834.
[52] M. Sethi, M. R. Knecht, *Langmuir* **2010**, *26*, 9860–9874.
[53] D. Xiang, X. Wang, C. Jia, T. Lee, X. Guo, *Chem. Rev.* **2016**, *116*, 4318–4440.
[54] N. Xin, J. Guan, C. Zhou, X. Chen, C. Gu, Y. Li, M. A. Ratner, A. Nitzan, J. F. Stoddart, X. Guo, *Nat. Rev. Phys.* **2019**, *1*, 211–230.
[55] M. Nyfeh, Manipulation and Patterning of Surfaces (Nanolithography) in *Fundamentals and Applications of Nano Silicon in Plasmonics and Fullerines* (Ed.: M. Nayfeh), Elsevier, **2018**, pp. 89–137.
[56] M. Manheller, S. Trellenkamp, R. Waser, S. Karthäuser, *Nanotechnology* **2012**, *23*, 125302.
[57] a) M. M. Deshmukh, A. L. Prieto, Q. Gu, H. Park, *Nano Lett.* **2003**, *3*, 1383–1385; b) G. Mészáros, S. Kronholz, S. Karthäuser, D. Mayer, T. Wandlowski, *Appl. Phys. A* **2007**, *87*, 569–575.
[58] J. Tang, Y. Wang, C. Nuckolls, S. J. Wind, *J. Vac. Sci. Technol. B* **2006**, *24*, 3227–3229.
[59] a) J. Liao, S. Blok, S. J. van der Molen, S. Diefenbach, A. W. Holleitner, C. Schonenberger, A. Vladyka, M. Calame, *Chem. Soc. Rev.* **2015**, *44*, 999–1014; b) T. Ishida, Y. Tachikiri, T. Sako, Y. Takahashi, S. Yamada, *Appl. Surf. Sci.* **2017**, *404*, 350–356.
[60] S. H. M. Jafri, A. Hayat, A. Wallner, O. Sher, A. Orthaber, H. Ottosson, K. Leifer, *Nanotechnology* **2020**, *31*, 225207.
[61] a) S. J. van der Molen, J. Liao, T. Kudernac, J. S. Agustsson, L. Bernard, M. Calame, B. J. van Wees, B. L. Feringa, C. Schönenberger, *Nano Lett.* **2009**, *9*, 76–80; b) Y. Viero, G. Copie, D. Guérin, C. Krzeminski, D. Vuillaume, S. Lenfant, F. Cleri, *J. Phys. Chem. C* **2015**, *119*, 21173–21183; c) D. Stiévenard, D. Guérin, S. Lenfant, G. Lévêque, C. A. Nijhuis, D. Vuillaume, *Nanoscale* **2018**, *10*, 23122–23130.
[62] Y. Yan, S. C. Warren, P. Fuller, B. A. Grzybowski, *Nat. Nanotechnol.* **2016**, *11*, 603–608.
[63] M. Segev-Bar, H. Haick, *ACS Nano* **2013**, *7*, 8366–8378.
[64] M. Manheller, S. Karthäuser, R. Waser, K. Blech, U. Simon, *J. Phys. Chem. C* **2012**, *116*, 20657–20665.
[65] M. Manheller, S. Karthäuser, K. Blech, U. Simon, R. Waser, in *Proceedings of 10th IEEE International Conference Nanotechnology (IEEE-Nano)*, Kintex, Korea, **2010**, pp. 919–923.
[66] a) Z. Lee, K.-J. Jeon, A. Dato, R. Erni, T. J. Richardson, M. Frenklach, V. Radmilovic, *Nano Lett.* **2009**, *9*, 3365–3369; b) S. Seo, M. Min, J. Lee, T. Lee, S.-Y. Choi, H. Lee, *Angew. Chem. Int. Ed.* **2012**, *51*, 108–112; *Angew. Chem.* **2012**, *124*, 112.
[67] J. Eklöf-Österberg, T. Gschneidtner, B. Tebikachew, S. Lara-Avila, K. Moth-Poulsen, *Small* **2018**, *14*, 1803471.
[68] K. S. Makarenko, Z. Liu, M. P. de Jong, F. A. Zwanenburg, J. Huskens, W. G. van der Wiel, *Adv. Mater.* **2017**, *29*, 1702920.
[69] C. Jia, A. Migliore, N. Xin, S. Huang, J. Wang, Q. Yang, S. Wang, H. Chen, D. Wang, B. Feng, Z. Liu, G. Zhang, D.-H. Qu, H. Tian, M. A. Ratner, H. Q. Xu, A. Nitzan, X. Guo, *Science* **2016**, *352*, 1443–1445.
[70] Q. Xu, G. Scuri, C. Mathewson, P. Kim, C. Nuckolls, D. Bouilly, *Nano Lett.* **2017**, *17*, 5335–5341.

Received: June 30, 2020